

# NONLINEAR SHALLOW WATER THEORIES FOR COASTAL WAVES

ERIC BARTHÉLEMY

*Laboratoire des Écoulements Géophysiques et Industriels,  
BP53, 38041 Grenoble Cedex 9, France  
E-mail: eric.barthelemy@hmg.inpg.fr*

(Received 1 June 2002; Accepted 20 October 2003)

**Abstract.** Ocean waves entering the near-shore zone undergo nonlinear and dispersive processes. This paper reviews nonlinear models, focusing on the so-called Serre equations. Techniques to overcome their limitations with respect to the phase speed are presented. Nonlinear behaviours are compared with theoretical results concerning the properties of Stokes waves. In addition, the models are tested against experiments concerning periodic wave transformation over a bar topography and of the shoaling of solitary waves on a beach.

**Keywords:** dispersion, harmonics, non-linear, Serre, shoaling, solitary waves, water waves

## 1. Introduction

Water waves propagating from deep water regions into water (of depth much less than their wavelength) experience significant transformations. Rapid changes in height, speed and direction produce considerable changes in free surface profiles. These profiles, initially almost sinusoidal, become characterized by long flat troughs, with crests appearing as isolated peaks. This change in shape is the so-called asymmetry. As depth decreases, waves become skewed about their crest with marked steepening of the forward face. Wave shoaling is the process that starts at the time when the waves first adapt to the bottom, progressing until they break.

Shallow water conditions are characterized by the water depth  $h_0$  being much smaller than the horizontal wave length scale  $L$  ( $L \sim 1/k$ ), where  $k$  is the wave number and is usually expressed by  $\sigma = kh_0 \ll 1$ . Within the linear approximation of water wave theory, the amplitude  $A$  is required to tend to 0 as  $L \rightarrow \infty$ . Obviously this implies that the scaling used in this linear approximation does not allow for shallow water waves of finite amplitude. Nonetheless the linear approximation indicates a quasi-uniform velocity with depth which is used in a number of approximate theories for long waves.

A widely accepted approach, starting with Boussineq (1872) and Rayleigh (1876), is a perturbation method based on two nondimensional



parameters  $\sigma$ , assumed small, and  $\epsilon = A/h_0$ . The smallness of  $\sigma$  is used to work out equations that do not depend on the vertical coordinate  $y$ . Moreover, the nonlinear free-surface conditions are absorbed in the resulting equations. These are usually easier to solve and, in simple cases, tractable analytically. Historically, these equations have been mostly dedicated to the study of solitary wave propagation.

The scalings generally adopted may severely restrict applicability to real world wave propagation problems. Indeed, shoaling waves start to transform when the wavelength is comparable with the depth ( $kh_0 \sim 1$ ). Moreover, waves will break when their amplitude is comparable with the depth ( $\epsilon \sim 1$ ). Thus, it is expected that classical scalings are unsuitable in large parts of the near-shore region. Deriving higher order equations to overcome such shortcomings will in most cases yield complex equations only amenable to numerical methods. These limitations have motivated the development of relatively simple methods encompassing waves of both short wavelength and of large amplitude.

In Section 2 the main steps of the derivation of a Boussinesq-like set of equations, incorporating high order nonlinear and dispersive terms, are presented. This set was originally obtained by Serre (1953). Section 3 presents a method to enhance dispersive behaviours of this set of equations. Finally, Section 4 is devoted to experimental test cases that were performed within the G8M-MAST II project of the European Commission.

## 2. A strongly nonlinear approximation: Serre equations for horizontal bed

### 2.1. NONDIMENSIONALISATION

The basic scales are the wave characteristic amplitude  $A$ , the wave characteristic horizontal length scale  $L$ , and the mean water depth  $h_0$ . Assuming that the waves' geometrical characteristic only depend on these scales, non-dimensional independent variables are naturally defined as follows:

$$x^* = \frac{x}{L} \quad \text{and} \quad y^* = \frac{y}{h_0}. \quad (1)$$

$y$  is the vertical coordinate and  $x$  is along the horizontal bottom. We know from the linear theory that the horizontal velocity  $u(x, y, t)$  has the following order of magnitude:

$$u \sim \epsilon C_0 \quad \text{with} \quad C_0 = \sqrt{gh_0}; \quad (2)$$

then the nondimensional horizontal velocity is,

$$u^* = \frac{u}{\epsilon C_0}, \quad (3)$$

where  $C_0$  is the long wave phase velocity. The order of magnitude of the vertical velocity is obtained using the continuity relation:

$$v \sim \sigma \epsilon C_0, \quad \text{thus } v^* = \frac{v}{\sigma \epsilon C_0} \quad (4)$$

Because we are dealing with long waves, the pressure is scaled by the static pressure,

$$p \sim \rho g h_0, \quad \text{thus } p^* = \frac{p}{\rho g h_0}. \quad (5)$$

The dimensionless form of continuity, irrotationality and, momentum equations and boundary conditions now read (\* dropped, for convenience):

$$u_x + v_y = 0 \quad (6)$$

$$u_y - \sigma^2 v_x = 0 \quad (7)$$

$$\epsilon u_t + \epsilon^2 (u^2)_x + \epsilon^2 (u v)_y = -p_x \quad (8)$$

$$\epsilon \sigma^2 v_t + \epsilon^2 \sigma^2 u v_x + \epsilon^2 \sigma^2 v v_y = -p_y - 1 \quad (9)$$

$$v = 0 \text{ at the horizontal bottom: } y = 0 \quad (10)$$

$$v = \eta_t + \epsilon u \eta_x \text{ at the free-surface: } y = h(x, t) = 1 + \epsilon \eta \quad (11)$$

$$p = 0 \text{ at the free-surface: } y = h(x, t) \quad (12)$$

## 2.2. DEPTH INTEGRATED EQUATIONS

Because in shallow water the horizontal component of the velocity is quasi-uniform over the depth, the depth averaged velocity is expected to be close to it. Depth averaged values are defined by

$$\bar{f} = \frac{1}{h} \int_0^h f \, dy \quad (13)$$

where  $h(x, t)$  is the total depth defined in Equation (11). The continuity Equation (6) integrated over depth gives

$$\eta_t + [h \bar{u}]_x = 0. \quad (14)$$

The momentum Equation (8) in the  $x$  direction is also depth averaged. Terms are simplified using the Leibnitz rule, the continuity Equation (14) and boundary conditions (10)–(12). After some manipulations Equation (8) reduces to:

$$\epsilon h \bar{u}_t + \epsilon^2 h \bar{u} \bar{u}_x + \epsilon^2 \frac{\partial}{\partial x} \int_0^h (u^2 - (\bar{u})^2) dy = - \int_0^h p_x dy. \quad (15)$$

The derivation so far is similar to that of Roseau (1976). The dispersion characteristic of the resulting equations will depend on the simplifying assumptions introduced for the pressure term of the right-hand side of Equation (15). If the pressure is assumed to be hydrostatic, then Equation (15) will result in the classical dispersionless shallow-water hyperbolic equations. Taking “on-board” dynamic pressure contributions gives dispersive behaviours. The Leibnitz rule applied to the right-hand term of (15) yields:

$$\int_0^h p_x dy = \frac{\partial}{\partial x} (h\bar{p}) - h_x p(h) = \frac{\partial}{\partial x} (h\bar{p}) \quad (16)$$

in which  $\bar{p}$  is computed as follows. The  $y$  momentum Equation (9) is rewritten as

$$-p_y = 1 + \epsilon \sigma^2 \Gamma(x, y, t) \quad (17)$$

$$\Gamma(x, y, t) = v_t + \epsilon uv_x + \epsilon vv_y, \quad (18)$$

where  $\Gamma$  is interpreted as the fluid particle vertical acceleration. Integrating (17) from  $y$  to  $h$  results in

$$-p(x, y, t) = (y - h) - \epsilon \sigma^2 \int_y^h \Gamma(x, \xi, t) d\xi. \quad (19)$$

Then,

$$-h\bar{p} = -\frac{1}{2}h^2 - \epsilon \sigma^2 \int_0^h dy \int_y^h \Gamma(x, \xi, t) d\xi. \quad (20)$$

The integral in the last term on the right-hand side is integrated by parts. Then Equation (15) reads

$$\bar{u}_t + \epsilon \bar{u} \bar{u}_x + \eta_x + \frac{\sigma^2}{h} \frac{\partial}{\partial x} \int_0^h y \Gamma(x, y, t) \, dy = -\frac{\epsilon}{h} \frac{\partial}{\partial x} \int_0^h (u^2 - (\bar{u})^2) \, dy. \tag{21}$$

Notice that Equation (21) is still exact. Hereafter approximations are introduced.

Using the fact that  $\sigma \leq 1$  in shallow water conditions, Rayleigh (1876), cited by Lamb (1932), expands the velocity potential in a Taylor series of  $y$ . The velocity potential is harmonic and because of the bottom kinematic condition (10), this expansion only contains even powers of  $y$ . Consequently the power series expansions of  $u$  and  $v$  (using irrotationality Equation (7)) are

$$u(x, y, t) = u^b(x, t) - \frac{1}{2} \sigma^2 y^2 \frac{\partial^2 u^b}{\partial x^2} + O(\sigma^4) \tag{22}$$

$$v(x, y, t) = -y \frac{\partial u^b}{\partial x} + \frac{1}{3!} \sigma^2 y^3 \frac{\partial^3 u^b}{\partial x^3} + O(\sigma^4), \tag{23}$$

where  $u^b$  is the horizontal bottom velocity. This is the starting point to compute  $\bar{u}$ ,  $\Gamma$  and  $(u^2 - (\bar{u})^2)$ . Depth averaging (22) results in

$$u^b = \bar{u} + \frac{1}{6} \sigma^2 h^2 \frac{\partial^2 \bar{u}}{\partial x^2} + O(\sigma^4, \epsilon \sigma^4) \tag{24}$$

$$u(x, y, t) = \bar{u} + \frac{1}{6} \sigma^2 h^2 \frac{\partial^2 \bar{u}}{\partial x^2} - \frac{1}{2} \sigma^2 y^2 \frac{\partial^2 \bar{u}}{\partial x^2} + O(\sigma^4, \epsilon \sigma^4). \tag{25}$$

The vertical velocity is

$$v(x, y, t) = -y \frac{\partial \bar{u}}{\partial x} + O(\sigma^2), \tag{26}$$

which substituted in (18) yields:

$$\Gamma = -y \overbrace{[\bar{u}_{xt} + \epsilon \bar{u} \bar{u}_{xx} - \epsilon (\bar{u}_x)^2]}^{\bar{G}(x,t)} + O(\sigma^2, \epsilon \sigma^2). \tag{27}$$

Note that  $h\bar{G}(x, t)$  is the free surface fluid particle vertical acceleration. Finally, it is straightforward to find that

$$\int_0^h (u^2 - (\bar{u}^2)) dy = O(\sigma^4, \epsilon\sigma^4). \quad (28)$$

The resulting evolution equations for  $\bar{u}$  and  $\eta$  are

$$\eta_t + [h\bar{u}]_x = 0 \quad (29)$$

$$\bar{u}_t + \epsilon \bar{u} \bar{u}_x + \eta_x - \frac{\sigma^2}{3h} \frac{\partial}{\partial x} (h^3 \bar{G}) = O(\sigma^4, \epsilon\sigma^4). \quad (30)$$

This set was originally derived by Serre (1953) by a very different procedure and, more than 10 years later, by Su and Gardner (1969). Extension to uneven bathymetries is given by Seabra-Santos et al. (1987), and used to predict free surface solitary waves passing a step, in comparison with experimental data. The range of validity of this set has been compared with the range of other nonlinear equations by Seabra-Santos et al. (1988). For a generalization to wave-current interactions and a very extensive review, the reader is referred to Dingemans (1997).

### 2.3. THE AIRY, BOUSSINESQ AND KDV APPROXIMATIONS

Depending on the order of magnitude of  $\epsilon$  compared with that of  $\sigma$ , different sets of equations can be deduced from (29) to (30). Ursell (1953) introduced a nondimensional parameter, the so-called Ursell number, that measures the relative strength of nonlinearity to dispersion. It is defined by

$$\text{Ur} = \frac{\epsilon}{\sigma^2} = \frac{AL^2}{h_0^3}. \quad (31)$$

#### 2.3.1. Airy's long wave theory

The simplest model retrieved, the Airy model, also known as the 1D shallow-water equations. It is often applied to the description of barotropic tides in coastal zones. Indeed the characteristic scales for tides are  $L = 10^3$  km,  $A = 1$  m and  $h_0 = 1$  km, implying that

$$\sigma^2 = 10^{-6} \ll \epsilon = 10^{-3} \ll 1 \quad \text{or} \quad \text{Ur} \gg 1. \quad (32)$$

Retaining terms up to order  $\epsilon$  in (29) and (30) gives

$$\eta_t + [h\bar{u}]_x = 0 \quad (33)$$

$$\bar{u}_t + \epsilon \bar{u} \bar{u}_x + \eta_x = 0 \quad (34)$$

The pressure distribution as given by Equation (19) reduces at the lowest order to a hydrostatic pressure distribution.

The set (33) and (34) is hyperbolic in nature and possess so-called weak solutions, such as shocks. This property can be used to describe the evolution of breakers inside the surf-zone (Keller et al., 1960; Ho and Meyer, 1962; Shen and Meyer, 1963a,b; Ho et al., 1963; Bonneten, 2001). The bore/shock induces an energy jump (dissipation). Other models of breaker evolution rely on an analogy with a hydraulic jump (Svendsen, 1984). Because the underlying assumptions in both approaches are identical (hydrostatic pressure, long waves), the predicted dissipated energy and the breaker evolution are comparable.

### 2.3.2. Boussinesq-like equations

Boussinesq equations can be derived in numerous ways. Whitham (1974), following the original derivation by Boussinesq (1872), uses a procedure involving the velocity potential. The approach given above based on the Euler equations is similar to that of Peregrine (1967). Let us suppose that

$$\sigma^2 \ll 1 \quad \text{but } \sigma^2 \sim \epsilon \text{ or } Ur \sim 1. \quad (35)$$

Thus, we retain in Equations (29) and (30) all terms of order  $\epsilon$  and  $\sigma^2$ , and neglect terms of order  $\epsilon\sigma^2 \sim \sigma^4$ . Most terms in the last term on the left-hand side of Equation (30) are discarded, and the set of equations written in dimensional form reduces to

$$\eta_t + [h \bar{u}]_x = 0 \quad (36)$$

$$\bar{u}_t + \bar{u} \bar{u}_x + g\eta_x = \frac{h_0^2}{3} \bar{u}_{xxt}. \quad (37)$$

The left-hand side is exactly the nonlinear nondispersive Airy long wave set. A dispersion term, however, appears on the right-hand side. The set (36) and (37) allows for waves propagating to the left and to the right. The most famous one-way propagation equation is the Korteweg–de Vries (KdV) equation proposed by Korteweg and de Vries (1895). Recasting the Boussinesq-like set (36) and (37) in a reference frame moving at  $C_0$ , and imposing slowly varying wave features, yields the KdV equation (Zauderer, 1989; Dingemans, 1997). A comparison of the evolution of a sinusoidal wave computed by Airy's theory with a computation based on the KdV equation is

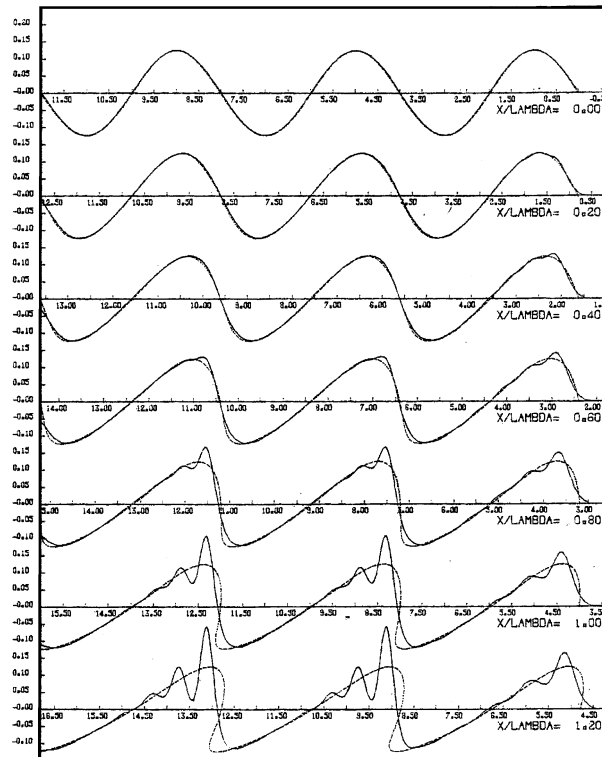


Figure 1. Evolution of a surface wave, sinusoidal at the start, from Airy's theory (---) and the KdV equation (—); plots of the surface displacement with time for various  $X$  locations are shown. Initial amplitude:  $A = 1.24$  cm; wavelength:  $LAMBDA = 3.96$  m; water depth:  $h_0 = 10.0$  cm; initial Ursell number  $Ur_0 = 39$  (Seabra-Santos, 1985).

given in Figure 1. It clearly emphasises that Airy's theory is only valid on short time scales. Detailed analysis of the time range validity can be found in Seabra-Santos et al. (1988) and Mei (1992). This numerical simulation shows the well known contribution of the dispersive term on the right-hand side in Equation (37). The initial steepening generates high harmonics, while the Airy equation tends to propagate these at the same speed, the KdV equation introduces a dispersion effect that produces undulating wave profiles. The higher the frequency the slower is the phase speed. Dispersion is known to balance nonlinearity to produce solitary waves.

### 2.3.3. The Serre equations (1953)

The Serre equations are simply the set (29) and (30). Keeping all terms implies that the amplitude of the waves is not small, that is  $\epsilon \sim O(1)$ . These equations, termed strongly nonlinear equations, contain all nonlinear

terms, including the convective vertical acceleration terms, and therefore can model highly nonlinear waves. This set written in dimensional form reads:

$$\eta_t + [h \bar{u}]_x = 0 \quad (38)$$

$$\bar{u}_t + \bar{u} \bar{u}_x + g\eta_x - \frac{1}{3h} \frac{\partial}{\partial x} [h^3 (\bar{u}_{xt} + \bar{u} \bar{u}_{xx} - (\bar{u}_x)^2)] = 0. \quad (39)$$

Apart from the leading nonlinearity,  $\bar{u}\bar{u}_x$ , these equations contain a wealth of other nonlinear terms. In contrast with the Boussinesq equation, the Serre equations have a solitary wave solution in closed form,

$$h(x, t) = h_0 + A \operatorname{sech}^2[K(x - Ct)] \quad (40)$$

$$\bar{u} = C \left( 1 - \frac{h_0}{h} \right) \quad (41)$$

$$K = \sqrt{\frac{3A}{4h_0^2(h_0 + A)}} \quad \text{and} \quad C = C_0 \sqrt{1 + \frac{A}{h_0}}. \quad (42)$$

$C$  is the phase speed of this steady, propagating wave whose shape does not change.  $K$  is the outskirt decay parameter (Shields and Webster, 1988). This solution is also known as the Rayleigh solitary wave solution. It reduces to the KdV solitary wave for small  $A/h_0$ . Guizien and Barthélemy (2002) use this solution to generate very stable solitary waves in flume experiments. Solitary waves (highly nonlinear) are used to assess nonlinear behaviours of different sets of equations. The increasing number of equations modelling nonlinear waves are found in the literature (Madsen and Schäffer, 1999; Wu, 2001) most of which are based on perturbation approaches developed here. Alternative methods, called direct approximations of the fluid motion with a free surface, have been derived by Green and Naghdi (1976) and Shields and Webster (1988). These are variational methods based on the reduction to ordinary differential equations, as given by Kantorovich and Krylov (1958).

### 3. Improving dispersion and nonlinear characteristics

Free surface motions containing a frequency spectrum result in ever changing free surface profiles in space and time. An inaccurate model for the phase speed (or dispersion characteristics) will produce shape distortion of the wave profiles. Phase speeds are given by dispersion relations which are investigated in the following on the basis of the linearised versions of the

sets derived above. Linearising Equations (36) and (37) and eliminating  $\eta$ , results in

$$\bar{u}_{tt} - C_0^2 \bar{u}_{xx} = \frac{h_0^2}{3} \bar{u}_{xxtt}. \quad (43)$$

In seeking solutions for  $\bar{u}$  of the form  $u_0 \exp i(kx - \omega t)$ , one obtains:

$$\omega^2 = \frac{k^2 C_0^2}{1 + \frac{1}{3}(kh_0)^2}. \quad (44)$$

Recalling the exact water wave dispersion relation (Airy–Stokes),

$$\omega^2 = gk \tanh kh_0, \quad (45)$$

dispersion relations (44) and (45) and that obtained using the KdV equation are plotted in Figure 2. It appears that, at high frequency, the waves tend to propagate at the wrong phase velocity. The higher the frequency the shorter are the waves, and consequently the larger  $\sigma^2 \simeq (kh_0)^2$ .

In the remainder of this Section a method for improving the dispersion behaviour of the long wave equations is presented. The method was

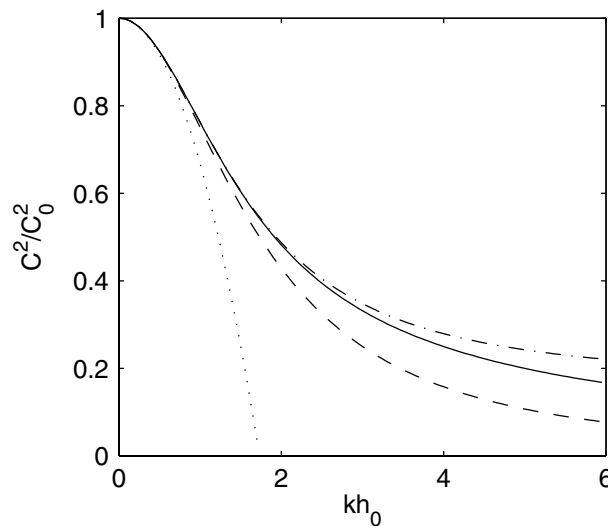


Figure 2. Dispersion relation:  $C^2/C_0^2$  as a function of  $kh_0$  (—): exact (45); (---): Boussinesq (44); (··): KdV; (-·-): improved Serre equations (50) with  $b = 1/15$ . Note that KdV even gives meaningless negative values of  $C^2$ .

initially suggested by Madsen et al. (1991). More recent developments can be found in Agnon et al. (1999), Madsen and Schäffer (1999) and Madsen et al. (2000).

Basically, the ideas are as follows. Because Equation (30) also reads

$$\bar{u}_t + \eta_x + \epsilon \bar{u} \bar{u}_x = O(\sigma^2, \epsilon \sigma^2), \tag{46}$$

it implies that

$$B(x, t) = bh_0^2[\bar{u}_{xxt} + g\eta_{xxx} + (\bar{u}\bar{u}_x)_{xx}] \tag{47}$$

is a small quantity of  $O(\sigma^4, \epsilon\sigma^4)$ . This term  $B$  is added (without any justification) to the right-hand side of either Equation (37) or (39), depending on which set one wishes to improve. It should be noted that the new set does not yield solitary wave solutions anymore. This new set reads:

$$\eta_t + [h\bar{u}]_x = 0 \tag{48}$$

$$\bar{u}_t + \bar{u}\bar{u}_x + g\eta_x = \frac{1}{3h} \frac{\partial}{\partial x} \left[ h^3 \left( \bar{u}_{xt} + \bar{u}\bar{u}_{xx} - (\bar{u}_x)^2 \right) \right] + B(x, t). \tag{49}$$

The dispersion behaviour of the linearized equation is investigated as previously to give

$$\frac{C^2}{C_0^2} = \frac{1 + b(kh_0)^2}{1 + (b + \frac{1}{3})(kh_0)^2}. \tag{50}$$

Going back to the exact linear dispersion relation, it is possible to write a [1/1] Padé approximation of it, which can be formally written as

$$\frac{C^2}{C_0^2} = \frac{1 + m(kh_0)^2}{1 + q(kh_0)^2}. \tag{51}$$

Comparing the Taylor expansions in  $kh_0$  of both Equations (45) and (51), at order  $(kh_0)^4$ , leads to

$$m = \frac{1}{15} \quad \text{and} \quad q = \frac{2}{5}. \tag{52}$$

The dispersion relation (50) is made close to the exact linear ones by choosing

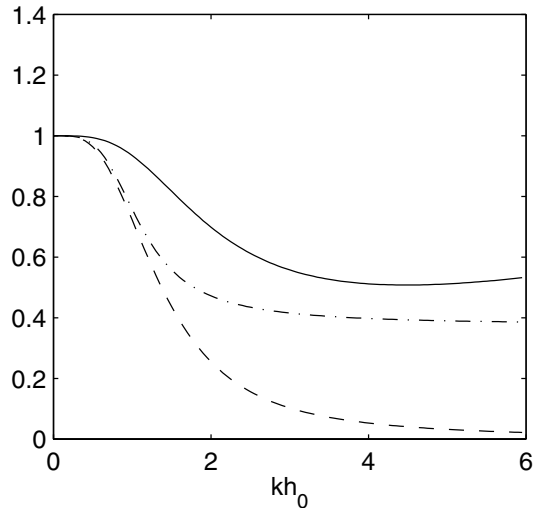


Figure 3. Stokes expansion analysis of the Serre equations. Amplitudes of the bound harmonics. (—):  $a_2/a_2^{\text{Stokes}}$ ; (- -):  $a_3/a_3^{\text{Stokes}}$ ; (- ·):  $\delta\omega/\delta\omega^{\text{Stokes}}$ .  $b = 1/15$ .

$$b = \frac{1}{15}. \quad (53)$$

In Figure 2 the relation (50) is plotted. An important improvement is noted. Mismatch with the exact relation at  $kh_0 = 6$  is roughly 10%. Once the value of  $b$  is chosen, the full equations can be integrated numerically. However, because of numerically induced dispersion it may be interesting to adjust  $b$  so that the linear dispersion behaviour of the numerical solution matches the exact linear one. Alternative corrections to the linear dispersion relation are presented by Whitman (1974, pp. 367–368 and 476–478) or Chester (1968). These are based on replacing the dispersive terms in the equation by a convolution integral that yields the exact Airy–Stokes dispersion relation (45).

As waves shoal when propagating towards the coast, the wave amplitudes increase; waves tend to become nonlinear. A precise prediction of the amplitude relies on accurate nonlinear properties of the models. Investigating the ability of models to propagate a weakly nonlinear Stokes waves is a straightforward test. A Stokes wave is a self-interacting wave with bound harmonics. Stokes analysis of nonlinear equations was initiated by Whitman (1974) on the KdV equation. It is easily generalized to other sets of equations (Madsen and Sorensen, 1993; Madsen and Schäffer, 1999). This type of analysis is related to the more general theory of polynoidal waves

(Boyd, 1990). The solution  $\bar{u}$  and  $\eta$  of the nonlinear equations are looked for as harmonic expansions of the following form:

$$\begin{aligned}\bar{u} &= u_1 \cos \theta + \epsilon u_2 \cos 2\theta + \epsilon^2 (u_3 \cos 3\theta + \delta u \cos \theta) \\ \eta &= a_1 \cos \theta + \epsilon a_2 \cos 2\theta + \epsilon^2 a_3 \cos 3\theta \\ \omega &= \omega + \epsilon^2 \delta\omega \\ \theta &= kx - \omega t\end{aligned}$$

Substituting these expressions into Equations (48) and (49) results in a hierarchy of algebraic problems with respect to  $\epsilon$ . The angular frequency  $\omega_0$  is naturally found to be given by Equation (51). The amplitudes of the harmonics are then

$$a_2 = \frac{3 a_1^2}{4 h_0} \frac{1}{(kh_0)^2} \left[ 1 + \left( \frac{1}{3} + 5b \right) (kh_0)^2 + \left( \frac{1}{3} b + 4b^2 \right) (kh_0)^4 + \dots \right] \quad (54)$$

$$a_3 = \frac{27 a_1^3}{64 h_0^2} \frac{1}{(kh_0)^4} \left[ 1 + \left( \frac{2}{3} + 15b \right) (kh_0)^2 + \left( \frac{1}{9} + \frac{35}{9} b + 63b^2 \right) (kh_0)^4 + \dots \right] \quad (55)$$

$$\delta\omega = \frac{9 a_1^2}{16 h_0} \frac{1}{(kh_0)^2} \left[ 1 + \left( 5b - \frac{1}{9} \right) (kh_0)^2 + \left( \frac{8}{27} + \frac{1}{3} b + 4b^2 \right) (kh_0)^4 + \dots \right]. \quad (56)$$

These expressions are plotted in Figure 3 in comparison with the Stokes solution as given by Whitham (1974, pp. 473–475). The latter reads:

$$a_2 = \frac{3 a_1^2}{4 h_0} \frac{1}{(kh_0)^2} \quad (57)$$

$$a_3 = \frac{27 a_1^3}{64 h_0^2} \frac{1}{(kh_0)^4} \quad (58)$$

$$\delta\omega = \frac{9 a_1^2}{16 h_0} \frac{1}{(kh_0)^2}. \quad (59)$$

It appears that the accuracy on the amplitude of the third harmonic decreases rapidly with  $kh_0$ , and the error exceeds 50% for  $kh_0 > 1.5$ . It should be noted that if the choice of  $b = 1/15$  is an optimum for the dispersion characteristics it is not necessarily one for the nonlinear behaviour.

#### 4. Experimental test cases

##### 4.1. SHOALING OF PERIODIC WAVES OVER BARRED-BEACHES

Submerged bars on beaches (breaking point sand bars, submerged breakwaters, coral reefs, etc.) are wide-spread bathymetric features. These induce wave modulations and transformations. While the waves shoal on the upstream slope of the bar, the amplitude increases, resulting in bound harmonic generation. This generation is an example of a triad interaction producing phase-locked harmonics. Passing the top, the waves encounter a sudden increase of water depth. In order to adjust, the bound harmonics are released as free waves. In turn triad interactions take place after the bar with the possibility of profile recurrence. Such decompositions have been also observed in the field (Byrne, 1969, Young, 1989).

Within the G8M-MAST II project, a blind test of models against experimental data (Luth et al., 1994) of wave interaction with a bar topography has been organised. The experiments were performed with an active wave absorber, also with compensation for bound long waves. These experiments had already been done by Beji and Battjes (1993), but on a linear scale of 1:2. The set up is shown in Figure 4. The experimental data used here are challenging since  $kh_0$  can be larger than 1 for the harmonics. An incorrect phase speed prediction in the models results in inaccurate free surface displacements. The LEGI model is run in comparison with these experimental data. The model includes improved frequency dispersion, but no nonlinear improvement (no  $(\bar{u}\bar{u}_x)_{xx}$  in  $B$ ). These equations are numerically integrated using the implicit finite difference scheme proposed by Mirie and Su (1982). The overall behaviour of the LEGI model against data can be evaluated in Figure 5. Measurements on the wave gauge at

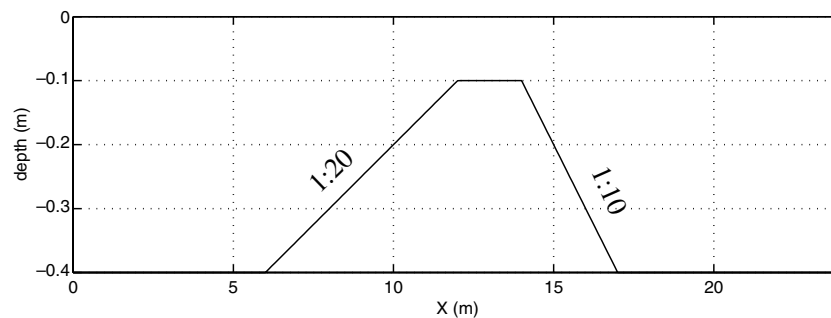


Figure 4. Layout the experimental bottom geometry. The depth 0 is the mean free surface position. Wave maker at  $X = 0$  m and active absorbing device at  $X = 25$  m (Dingemans, 1994; Luth et al., 1994).

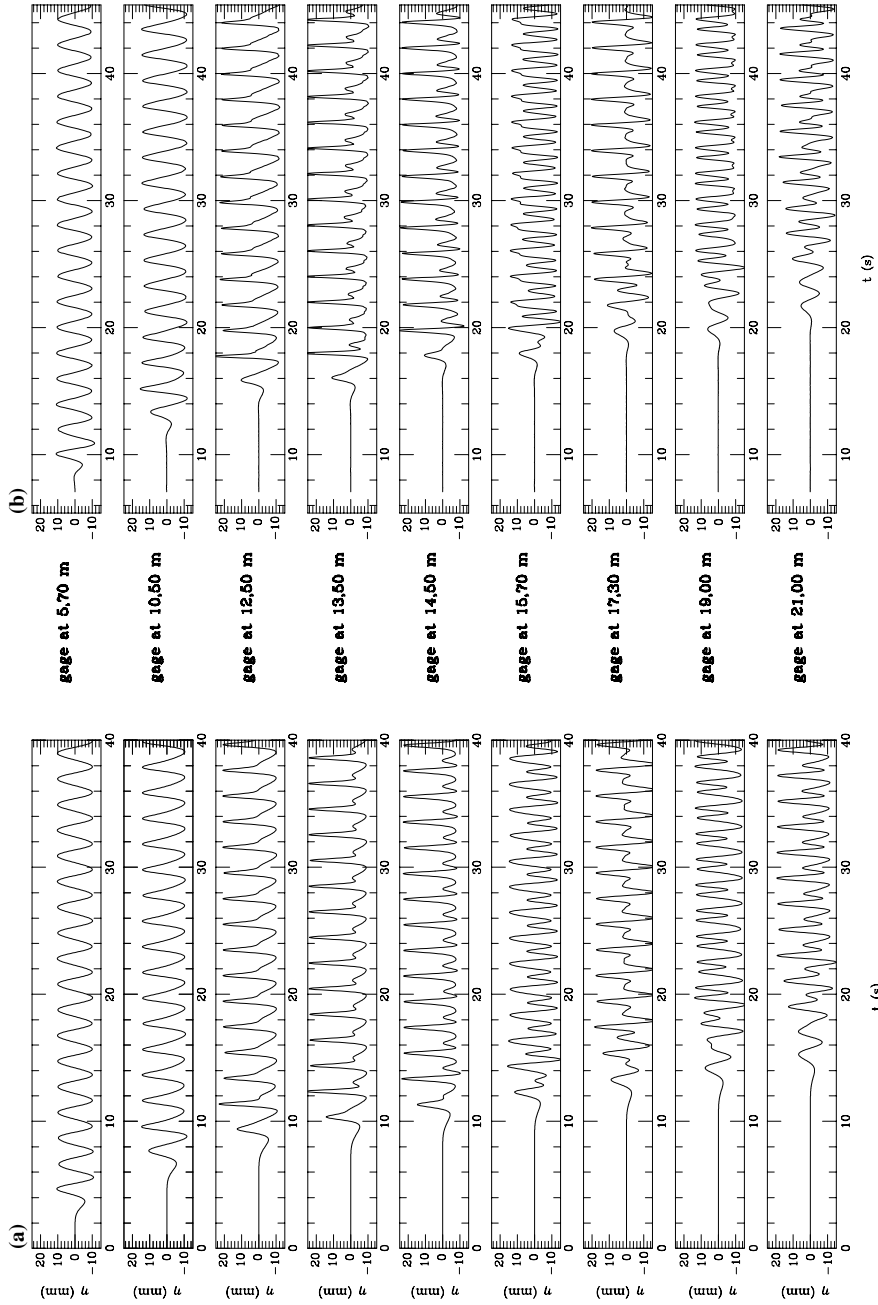


Figure 5. Surface displacements (in mm) with time (in seconds) at various locations along the flume. (a) LEGI Serre model with  $b = 1/15$ . (b) Flume experiments of Beji and Battjes (1993). Test case A:  $T = 2.02$  s,  $A = 1$  cm.

$x = 5.7$  m show that the wave is quasi sinusoidal. Secondary crests in the free surface elevation is also a pre-eminent feature due to the presence of higher harmonics.

The performance of the LEGI model (extension of (48) and (49) to uneven bottom), is given for three different test cases in Figures 6–8. Notice that only the recordings for the probes located after the bar are plotted. (In the shoaling process (before the top of the bar) the discrepancies between models and data are much less than after).

The LEGI model improved dispersion characteristics behaves reasonably well for test case A, for which  $a_1 \simeq 0.0175$  m,  $a_2 \simeq 0.025$  m and  $a_3 \simeq 0.0125$  m after the bar (values from Madsen and Schäffer, 1999). These plots also clearly emphasise that, with  $b=0$ , the profiles bear little resemblance with measurements. Performance of the model against test case B is not as good since it is a more nonlinear case than A even though the harmonics are of similar wavelength. For case B, the amplitudes are overestimated and free surface profiles not at all alike. Test case C is a strong

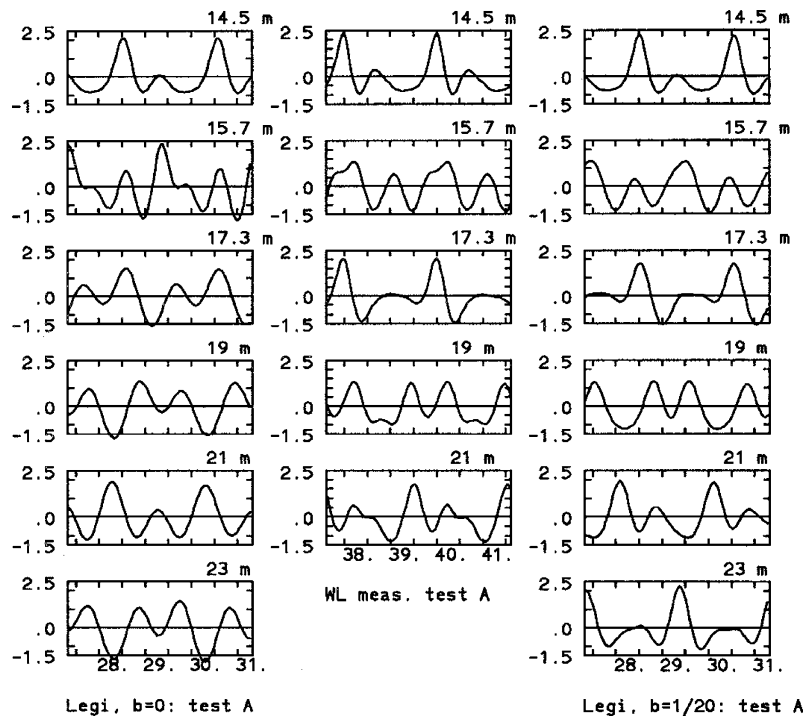


Figure 6. Enlargements of the surface displacements (in cm) with time (in seconds) at various locations after the bar. Test case A:  $T = 2.02$  s,  $A = 1$  cm. In the deeper parts of the flume:  $\epsilon = 0.025$  and  $kh_0 = 0.67$ . Left-hand column: simulations without dispersion enhancement ( $b = 0$ ). Central column: flume measurements. Right-hand column: simulations with dispersion enhancement ( $b = 1/20$ ).

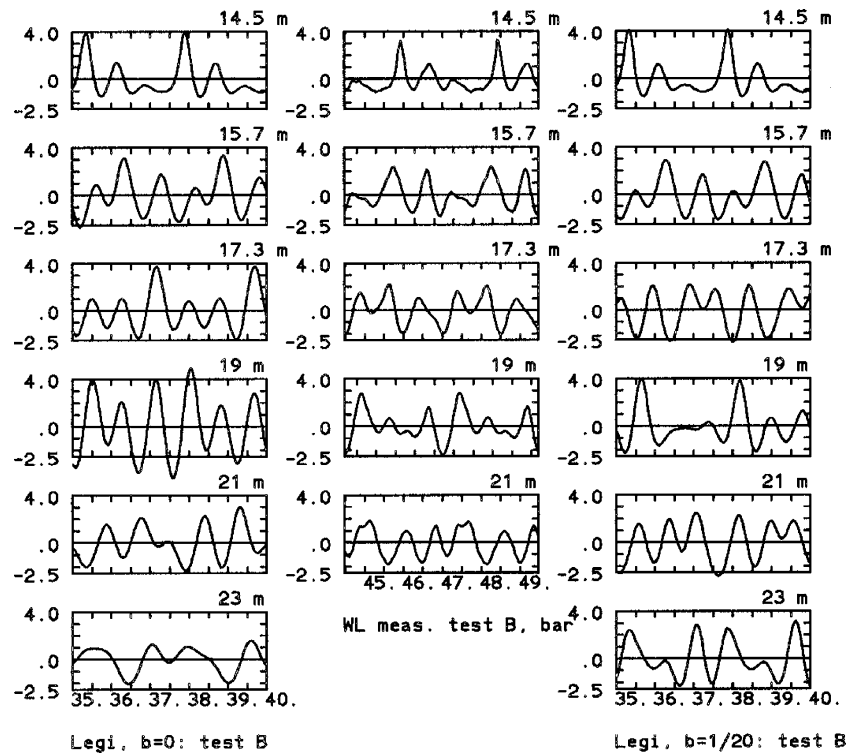


Figure 7. Enlargements of the surface displacements (in cm) with time (in seconds) at various locations after the bar. Test cast B:  $T = 2.525$  s,  $A = 1.45$  cm. In the deeper parts of the flume:  $\epsilon = 0.036$  and  $kh_0 = 0.52$ . Left-hand column: simulations without dispersion enhancement ( $b = 0$ ). Central column: flume measurements. Right-hand column: simulations with dispersion enhancement ( $b = 1/20$ ).

nonlinear case for shorter waves than A and B (half the wave period). This test case combines both a high value  $kh_0$  and large amplitudes,  $a_1 \simeq 0.05$  m,  $a_2 \simeq 0.0125$  m and  $a_3 \simeq 0.00251$  m. According to Figure 3 the error on the amplitude of the second harmonic is roughly 40% smaller than it should be and even 90% for the third harmonic. Consequently, the numerics tend to predict a quasi-sinusoidal wave. Incorporation of higher order  $O(\epsilon\sigma^4)$  nonlinear terms in the equations improves the prediction (Madsen and Schäffer, 1999) but the draw back is numerically cumbersome equations.

#### 4.2. SOLITARY WAVE SHOALING

It has long been observed (Munk, 1949) that waves running up a beach become narrower and that the crests behave as dynamically independent waves. Crests are very sharp and their spacing large, so they look like solitons. Shoaling waves interact very weakly as shown by Stiassnie and

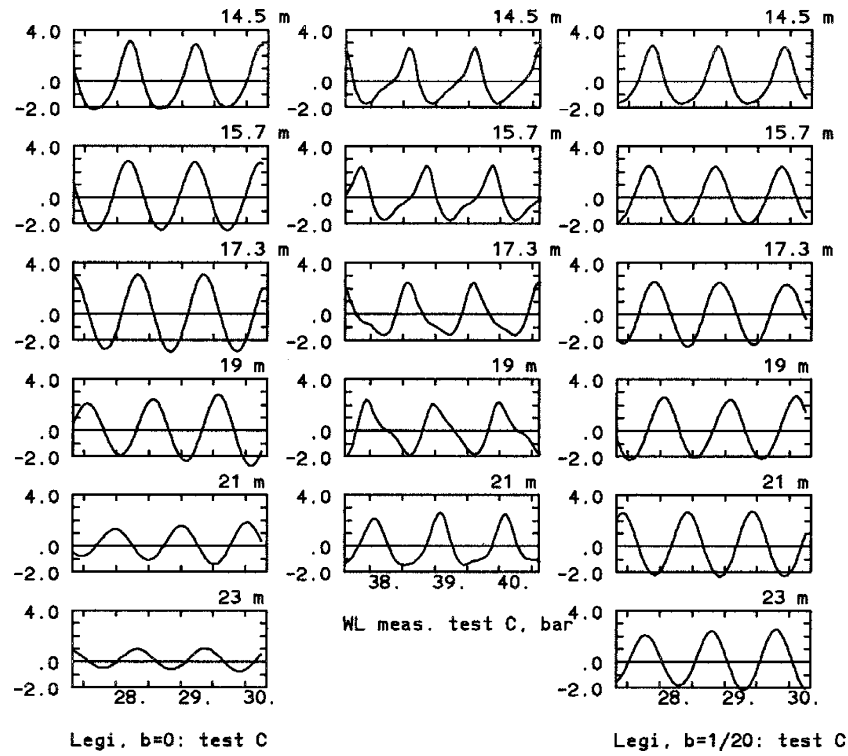


Figure 8. Enlargements of the surface displacements (in cm) with time (in seconds) at various locations after the bar. Test case  $C:T = 1.01$  s,  $A = 2.05$  cm. In the deeper parts of the flume:  $\epsilon = 0.050$  and  $kh_0 = 1.69$ . Left-hand column: simulations without dispersion enhancement ( $b = 0$ ). Central column: flume measurements. Right-hand column: simulations with dispersion enhancement ( $b = 1/20$ ).

Peregrine (1980). Consequently, the shoaling of solitary waves is a good test of model nonlinear capability. Shoaling of finite amplitude waves inevitably results in breaking. The prediction of the crest amplitude evolution is of importance in coastal morphodynamics, since crest velocity determines the magnitude of sand transport and therefore eventually the underwater sand bar formation.

Experiments were performed in the LEGI 36 m long linear glass flume (Guibourg and Barthélemy, 1994). It is equipped with a piston wavemaker. Free surface displacements are measured with resistive type probes (resolution of 0.1 mm). Data on solitons shoaling on plane beaches of slopes 1/7.6, 1/11.43, 1/14.92, 1/30 and 1/60 were collected. We focus here on how the Serre equations perform in comparison with the Boussinesq equations in terms of wave profiles and crest amplitude prediction on the 1/60 beach slope experiments. The models used are extensions of the Serre equations (Seabra-Santos et al., 1987) and the Boussinesq equations (36) and (37) to uneven topographies and without improved dispersion.

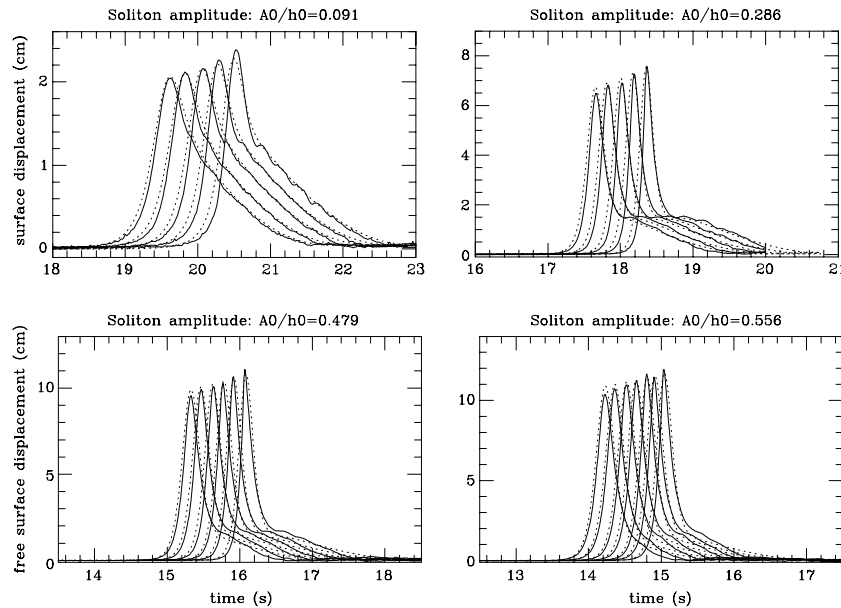


Figure 9. Free surface displacements against time (in seconds) for a shoaling solitary wave at various locations. Beach slope of 1/60. (—) flume measurements; (---) numerical simulations by the Serre equations.  $A_0$  is the amplitude of the solitary wave at the toe of the beach and the  $h_0$  the uniform depth before the beach.

In Figure 9 wave profiles are reproduced in a satisfactory way by the Serre equations, with respect to both the skewness and the crest amplitude.

Close inspection of Figure 10, however, shows that the Boussinesq equations tend to overestimate crest amplitude evolution  $A/A_0$  by up to 15%. In Figure 10 the classical Green's law derived from energy conservation for linear long waves is also plotted. This law is

$$\frac{A}{A_0} = \left( \frac{h}{h_0} \right)^{-\frac{1}{4}}. \quad (60)$$

As expected, for large initial amplitudes, this linear approximation is highly inaccurate.

## 5. Conclusions

We have presented a series of one-dimensional nonlinear models ranging from weakly nonlinear to strongly nonlinear for the study of water waves in near-shore environments. Amongst those the Serre equations are more

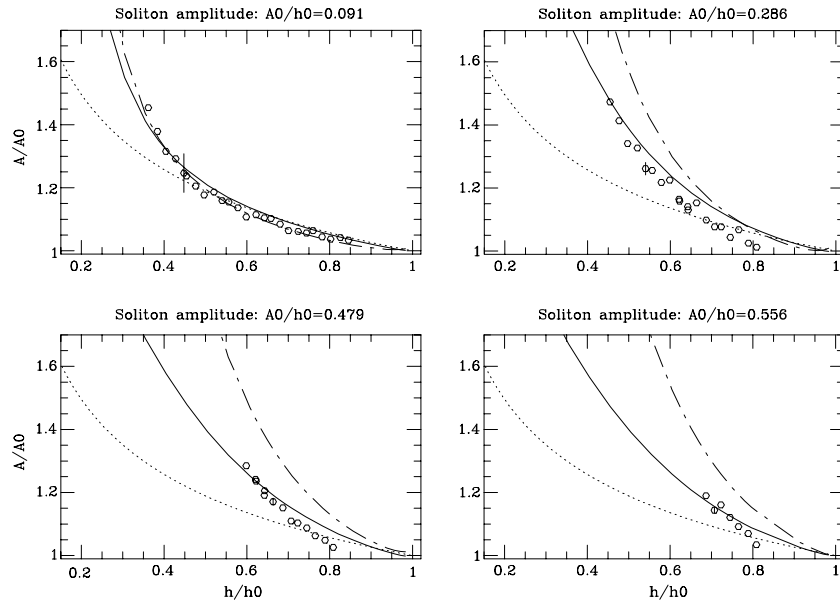


Figure 10. Wave peak amplitude  $A$  evolution along the beach.  $h$  is the depth at a given position on the beach. (o) Flume measurements; (—) numerical simulations by the Serre equations; (— —) numerical simulations by the Boussinesq equations; (· · ·) Green's law, equation (60).

deeply discussed. In principle, the latter set of equations contains more nonlinear “information” than the standard Boussinesq sets. Improvements of the dispersion characteristics in the range of shorter waves  $kh_0 \geq 1$  are also discussed. Comparisons with theoretical solutions, such as the exact dispersion relation or the nonlinear Stokes waves (third order), are presented. Serious limitations in this latter case are pointed out. Numerical phase speeds can be adjusted without much effort to match closely the exact dispersion relation for a wide range of  $kh_0$ , but this is not so for the nonlinear characteristics such as the first and second harmonic amplitude. However, tests on long wave shoaling in comparison with experiments show that the Serre equations are able to predict reliable peak amplitudes. This is a crucial point to locate correctly the breaking point of the waves and the sediment transport in the shoaling zone.

Dispersion behaviour may also be improved by rewriting the Serre equations (38) and (39) in terms of the velocity  $u$  at an arbitrary level, chosen in order to match as well as possible the exact dispersion relation (see Witting, 1984). Moreover, the nonlinearity can be further improved by incorporating terms of  $O(\epsilon\sigma^4)$  neglected in eq. (30), as achieved by Madsen and Schäffer, (1999) or by reconsidering the nonlinear problem as a time marching problem (Agnon et al., 1999, Madsen et al., 2000). Extensions to

two-dimensional flows to allow for wave refraction on beaches are of practical importance, but have not been discussed here. For the incorporation of wave breaking and breaker evolution into models, the reader is referred to Madsen et al. (1997a,b).

### Acknowledgements

This work was initially funded by the European Commission under CEC MASTII contract MAS2-CT92-0027. The author wishes to acknowledge with thanks the support provided by EU. Many thanks to the organizing committee of the Grand Combin Summer School that made this paper possible.

### References

- Agnon, Y., Madsen, P. A., and Schäffer, H. A.: 1999, 'A New Approach to High-order Boussinesq Models', *J. Fluid Mech.* **399**, 319–333.
- Beji S. and Battjes, J. A.: 1993, 'Experimental Investigations of Wave Propagation Over a Bar', *Coastal Eng.* **19**, 151–162.
- Bonneton, P.: 2001, 'A Note on Wave Propagation in the Inner Surf-zone', *C. R. Acad. Sci.-Paris* **239** (1), 27–33.
- Boussinesq, J.: 1872, 'Théories de ondes et des remous qui se propagent le long d'un canal rectangulaire, en communiquant au liquide contenu dans ce canal, des vitesses sensiblement pareilles de la surface au fond', *J. Math. Pures Appl. 2ième Sér.* **17**, 55–108.
- Boyd, J. P.: 1990, 'New Directions, in Solitons and Non-linear Periodic Waves: Polycnoidal Waves, Imbricated Solitons, Weakly Nonlocal Solitary Waves, and Numerical Boundary Value Algorithms', *Adv. Appl. Mech.* **27**, 1–82.
- Byrne, R. J.: 1969, 'Field Occurrences of Induced Multiple Gravity Waves', *J. Geophys. Res.* **23**, 1–16.
- Chester, W.: 1968, 'Resonant Oscillations of Water Waves. I. Theory', *Proc. R. Soc. A.* **306**, 5–22.
- Dingemans, M. W.: 1994, *Comparison of Computation with Boussinesq-like Models and Laboratory Measurements*, Technical report, Delft Hydraulics, MAST-G8M Note H1684.
- Green, A. E. and Naghdi, P. M.: 1976, 'A Derivation of Equations for Wave Propagation in Water of Variable Depth', *J. Fluid Mech.* **78**, 237–246.
- Guibourg, S. and Barthélemy E.: 1994, 'Long Wave Equations. A Comparison with Experimental Shoaling on Plane Beaches', in: *Modelling of Coastal and Estuarine Processes*, Séminaire Franco-Portugais de Modélisation en Hydraulique Maritime, Coimbra, pp. 83–92.
- Guizien, K. and Barthélemy E.: 2002, 'Accuracy of Solitary Wave Generation by a Piston Wave Maker', *J. Hydr. Res.* **40**(3), 321–331.
- Ho, D., Meyer, R. E. and Shen, M. C.: 1963, 'Long Surf', *J. Marine Res.* **21**(3), 219–233.
- Ho, D. V. and Meyer, R. E.: 1962, 'Climb of a Bore on a Beach. Part I. Uniform Beach Slope', *J. Fluid Mech.* **14**, 305–318.

- Kantorovich, L. V. and Krylov, V. I.: 1958, *Approximate Methods of Higher Analysis*. Groningen, P. Noordhoff Ltd, The Netherlands.
- Keller, H. B., Levine, D. A., and Whitham, G. B.: 1960, 'Motion of a Bore over a Sloping Beach', *J. Fluid Mech.* **7**, 302–316.
- Korteweg, D. J. and de Vries, G.: 1895, 'On the Change of Form of Long Waves Advancing in a Rectangular Canal, and on a New Type of Long Stationary Waves', *Philos. Mag. J. Sci.* **39**, 422–443.
- Lamb, H.: 1932, *Hydrodynamics*, 6th ed., Cambridge: Cambridge University Press.
- Luth, H. R., Klopman, G., and Kitou, N.: 1994, *Project 13G: Kinematics of Waves Breaking Partially on an Offshore Bar; LDV Measurements for Waves With and Without a Net Onshore Current*, Technical report, Delft Hydraulics. Technical Report H1573.
- Madsen, P. A., Bingham, H. and Hua, L.: 2000, 'The Ultimate Boussinesq Formulation for Highly Dispersive and Highly Nonlinear Water Waves', in: *Proceedings of the 27th International Conference on Coastal Engineering*, pp. 176–189.
- Madsen, P. A., Murray, R., Sorensen, and O. R.: 1991, 'A New Form of the Boussinesq Equations with Improved Linear Dispersion Characteristics', *Coastal Eng.* **15**, 371–388.
- Madsen, P. A. and Schäffer, H. A.: 1999, 'A Review of Boussinesq -type Equations for Surface Gravity Waves', in P. Liu (ed.), *Advances in Coastal and Ocean Engineering*, Vol. 5, World Scientific, pp. 1–94.
- Madsen, P. A. and Sorensen, O. R.: 1993, 'Bound Waves and Triad Interactions in Shallow Water', *Ocean Eng.* **20**, 359–388.
- Madsen, P. A., Sorensen, O. R. and Schäffer, H. A.: 1997a, 'Surf Zone Dynamics Simulated by a Boussinesq Type Model. Part I. Model Description and Cross-Shore Motion of Regular Waves', *Coastal Eng.* **32**, 255–288.
- Madsen, P. A., Sorensen, O. R., and Schäffer, H. A.: 1997b, 'Surf Zone Dynamics Simulated by a Boussinesq Type Model. Part II. Surf Beat and Swash Oscillations for Wave Groups and Irregular Waves', *Coastal Eng.* **32**, 289–320.
- Mei, C. C.: 1992, *Applied Dynamics of Ocean Surface Waves*, 2nd ed., World Scientific, Singapore.
- Mirie, R. M. and Su, C. H.: 1982, 'Collision Between Two Solitary Waves . Part 2. A Numerical Study', *J. Fluid Mech.* **115**, 475–492.
- Munk, W. H. : 1949, 'The Solitary Wave and its Application to Surf Problems', *Ann. New York Acad. Sci.* **51**, 376–424.
- Peregrine, D. H.: 1967, 'Long Waves on Beaches', *J. Fluid Mech.* **27**(4), 815–827.
- Rayleigh, L.: 1876, 'On Waves', *Philos. Mag. J. Sci. Ser. 5* **1** (4), 257–279.
- Roseau, M.: 1976, *Asymptotic Wave Theory, in Series in Applied Mathematics and Mechanics*, Vol. 20, North-Holland Publishing Company, Amsterdam.
- Seabra-Santos, F. J.: 1985, *Contribution à l'étude des ondes de gravité bidimensionnelles en eau peu profonde*. Ph.D. Thesis, Institut National Polytechnique de Grenoble et Université Scientifique et Médicale de Grenoble 1.
- Seabra-Santos, F. J., Renouard, D. P., and Temperville, A. M.: 1987, 'Numerical and Experimental Study of the Transformation of a Solitary Wave over a Shelf or Isolated Obstacle', *J. Fluid Mech.* **176**, 117–134.
- Seabra-Santos, F. J., Renouard, D. P., and Temperville, A. M.: 1988, 'Etude théorique et expérimentale des domaines de validité des théories d'évolution des ondes en eau peu profonde', *Annales Geophysicae* **6**(6), 671–680.
- Serre, F.: 1953, 'Contribution à l'étude des écoulements permanents et variables dans les canaux', *Houille Blanche* **8**, 374–388.
- Shen, M. C. and Meyer, R. E.: 1963a, 'Climb of Bore on a Beach. Part II. Non-Uniform Beach Slope', *J. Fluid Mech.* **16**, 108–112.

- Shen, M.C. and Meyer, R. E.: 1963b, 'Climb of a Bore on a Beach. Part III. Run up', *J. Fluid Mech.* **16**, 113–125.
- Shields, J. J. and Webster, W. C.: 1988, 'On Direct Methods in Water Wave Theory' *J. Fluid Mech.* **197**, 171–199.
- Stiassnie, M. and Pegerine, D. H.: 1980, 'Shoaling of Finite Amplitude Surface Waves on Water of Slowly Varying Depth', *J. Fluid Mech.* **97**, 783–780.
- Su, C.H. and Gardner, C. S.: 1969, 'KDV Equation and Generalizations. Part III. Derivation of Korteweg-de Vries Equation and Burgers Equation', *J. Math. Phys.* **10**(3), 536–539.
- Svendsen I. A.: 1984, 'Wave Heights and Set-Up in a Surf Zone', *Coastal Eng.* **8**(4), 303–329.
- Ursell, F.: 1953, 'The Long -Wave Paradox in the Theory of Long Gravity Waves', *Proc. Camb. Philos. Soc.* **49**, 685–694.
- Whitham, G. B.: 1974, *Linear and Non-Linear Waves*, John Wiley and Sons, New-York.
- Witting, J. M.: 1984, 'A Unified Model for the Evolution of Non-linear Waves', *J. Comput. Phys.* **56**, 203–236.
- Wu, T. Y.: 2001, 'A Unified Model for Modelling Water Waves', *Adv. Appl. Mech.* **37**, 1–88.
- Young, I. R.: 1989, 'Wave Transformation Over Coastal reefs', *J. Geophys. Res.* **94**, 9779–9789.
- Zauderer, E.: 1989, *Partial Differential Equations of Applied Mathematics*, Pure and Applied Mathematics, 2nd ed., John Wiley & Sons.